doi:10.1038/nature10309

Table of Contents:

1. Magnetic configuration of the Co dots

Representative magnetization curves of a 500 nm device are shown in Fig. S1. The hysteresis curves show that the AlO_x/Co/Pt samples present strong perpendicular anisotropy, with out-of-plane easy axis (θ = 0º), as expected from previous work[1-4]. Field-driven magnetization reversal in dots as large as 200-500 nm likely occurs following sudden domain nucleation and propagation, as shown by the abrupt change of sign of M_z in Fig. S1a and b. Minor loop measurements, reported in Fig. S2a for a different sample, show that, in the absence of steps, the AHE signal is always reversible, with a remanent R_{Hall} equal to that measured for a uniform perpendicular monodomain state. This indicates that applied fields having a nonzero vertical component (typically corresponding to θ ≤ 89º and θ ≥ 91º with ± 1º accuracy) uniformly tilt the magnetization along the in-plane direction. On the other hand, for very well-aligned in-plane fields (θ = 90º) we observe that the AHE signal varies in steps, indicating that M_z breaks into multiple domains. Minor field loops beyond such steps show hysteretic behavior (Fig. S2b).

By measuring switching curves for different field angles θ we can assess the influence of magnetic domains on the current-induced reversal mechanism. The measurements reported in Fig. 1 and 2 of the main text are performed for a uniformly tilted magnetization state. The tilt angles can be estimated from the decrease of the AHE signal

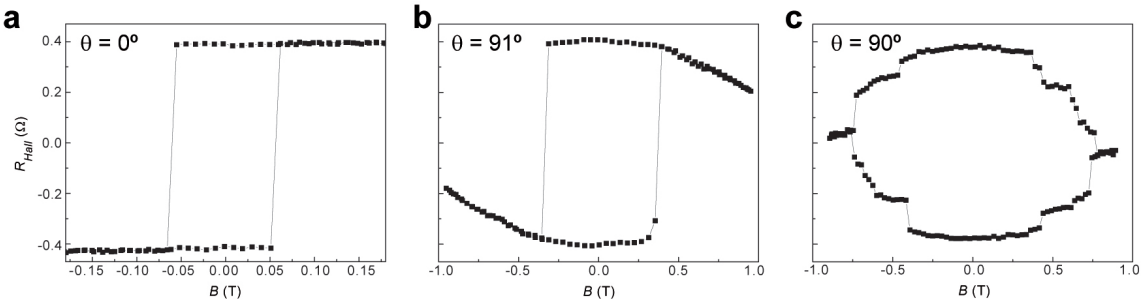

Figure S1. Hysteresis curves of a 500 nm Co dot. **a,** M_z measured as a function of magnetic field (B) applied perpendicular to the sample surface (θ = 0º). **b,** Measurements taken close to the hard plane direction (θ = 91º) show the expected increase in coercivity. **c,** When B is aligned to the hard plane (θ = 90º) M_z breaks into domains, as shown by the discrete jumps of the anomalous Hall resistance. All measurements were performed at room temperature using a dc current of 110 μA.

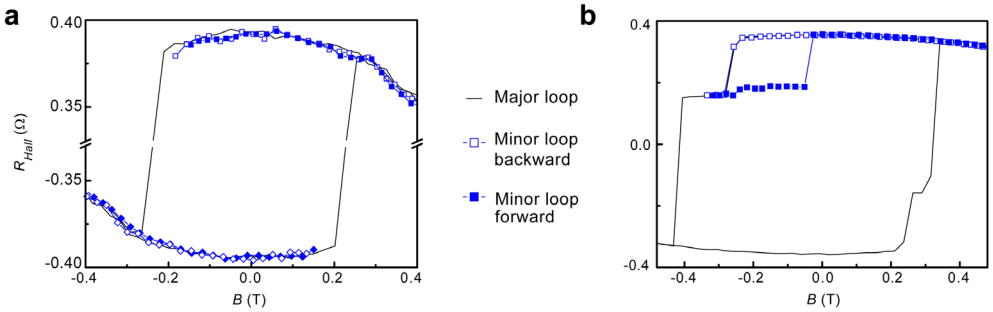

Figure S2. a, Hysteresis cycle with magnetic field aligned slightly off-plane (θ = 84º). Minor field loops (blue symbols) show reversible magnetization behavior. **b,** Hysteresis cycle with magnetic field aligned close to in-plane (θ = 89º) and hysteretic minor loop.

for increasing applied field (see, e.g., Fig. S2a), and are typically comprised between 3º and 15º for B_x ranging from 0.05 and 0.3 T. Figure S3 shows a switching curve obtained at θ = 90º in the presence of magnetic domains. Switching occurs between the equilibrium multi-domain states stabilized by the planar field (cfr. Fig. S1c and S3). However, the symmetry and force of the switching effect remain unchanged, independently of the presence of magnetic domains and domain walls. Further proof that this phenomenon is robust with respect to changes of the magnetic configuration is its reproducibility from sample to sample. Whereas we expect differences in the nucleation fields and propagation velocity of domains, known to be dominated by material in-homogeneities or sample shape, we measure reproducible switching from sample to sample and even in samples of different size and shape. These observations reinforce the analogy between the effect that we report

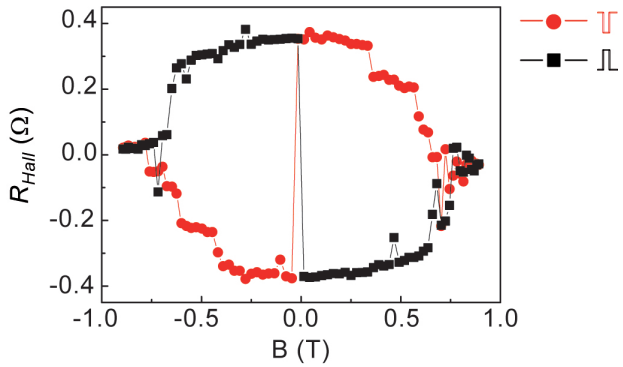

Figure S3. Current-induced switching with magnetic field aligned in-plane (θ = 90º, ϕ = 0º) of the sample measured in Fig. S1. M_z is measured by AHE after injection of positive (black squares) and negative (red circles) current pulses of amplitude I_p = 2.58 mA.

here and an effective perpendicular magnetic field: similar to an external field, the perpendicular component of the effective spin-orbit field is able to reverse the magnetization independently from the magnetic configuration of the sample.

2. Switching dependence on the current pulse length

The relationship between switching current amplitude and pulse length (τ_p) provides clues about the role played by thermal fluctuations in the magnetization reversal process. As seen in Fig. 2, the critical current for switching devices of 500 nm lateral size is around 1.9 mA for 15 ns long pulses. This value, assuming a 3.6 nm thick lateral interface (Pt+Co), corresponds to a current density of about 10^8 A/cm^2. In order to measure the dependence of driving current on τ_p, however, we define a higher current threshold (I_c), for which 100% switching probability is obtained all the way up to $B = B_c$. Figure S4a shows I_c measured as a function of τ_p in the 10 to 100 ns range. The same data are plotted as a function of inverse pulse length in Fig. S4b. We observe that I_c decreases linearly with τ_p^{-1} up to pulse lengths of the order of 30 ns. For longer pulses, this linearity disappears and the decrease of I_c with τ_p^{-1} becomes more significant. It is interesting to remark that a similar behavior was observed in the context of spin transfer torque[5,6]. In trilayer spin valve structures, the linear dependence of current amplitude on switching speed is typical of a supercritical region

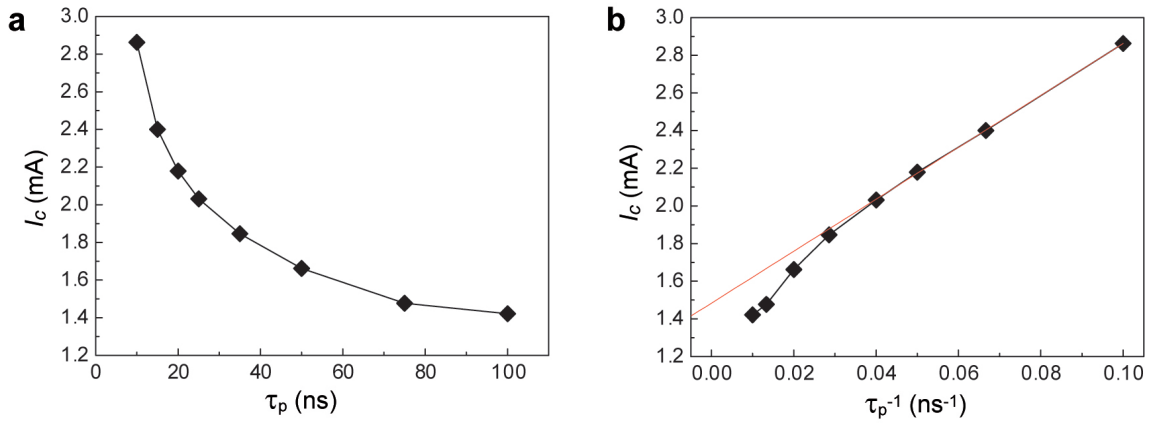

Figure S4. Dependence of the critical switching current on **a,** current pulse length and **b,** inverse pulse length. The red line is a linear fit to the data for $\tau_p < 30$ ns. I_c is defined as the current threshold for which complete switching is observed for one pulse within the entire bistability range of the Co dot.

where the temperature (including current-induced heat) induces random deviations of the magnetization from its equilibrium direction, thus favoring the action of a spin torque. In the subcritical region, a finite temperature directly favors the switching process as the probability for thermally activated magnetization reversal increases. Since this behavior follows from quite general assumptions based on the conservation of angular momentum and the action of random thermal perturbations[5], we believe that the data of Fig. S4 can be explained using a similar model, even though the spin torque origin is different.

3. Switching dependence on the lateral size of the Co dot

In order to prove that the absolute critical current necessary to induce controlled magnetization reversal scales with the lateral sample size, we have fabricated a 200 nm square Co dot device and carried out switching measurements as a function of current. The results, shown in Fig. S5, are similar to those reported for the larger devices, but the critical current has now decreased by almost a factor 2, proportionally to the decrease of the lateral dot surface at constant current density. We note that, due to the strong magnetic anisotropy of Al/Co/Pt layers[1-4], further size reduction of the device is possible without compromising the thermal stability of the magnetization at room temperature.

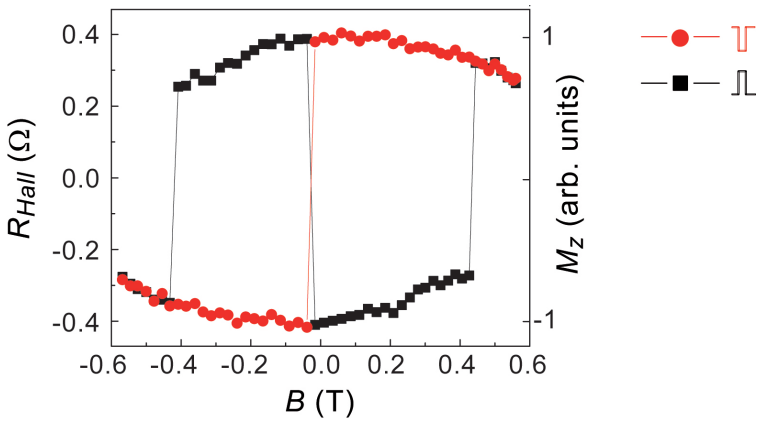

Figure S5. Current-induced switching of a 200 nm Co dot. M_z is measured by the anomalous Hall resistance after injection of positive (black squares) and negative (red circles) current pulses of amplitude I_p = 1.38 mA. The data are reported as a function of a nearly in-plane magnetic field B (θ = 92°) aligned to the current direction (ϕ = 0°).

4. Estimation of the effective switching field

To estimate the magnitude of the effective perpendicular switching field induced by the current, we have measured the probability of switching as a function of current in the presence of an applied field with constant in-plane component (B_x = 100 mT) and variable perpendicular component (B_z = -7 - 7 mT). Depending on the current polarity, B_z either favours or opposes the reversal of M_z.To perform this measurement, we alternate current pulses of opposite polarity: the amplitude of the first pulse is fixed at a value that ensures successful switching while the second one is gradually increased. This sequence is repeated twenty times for each value of the applied field and pulse amplitude. The average of M_z following the second pulse is plotted in Fig. S6 as a function of field and current. This method reveals the gradual onset of switching as a function of current density for different perpendicular magnetic fields. The red area designates successful switching, while blue represents failed switching. Using such data one can estimate the approximate intensity of the effective field from the slope of the critical current vs. B_z. This estimate yields a value of approximately 70-90 mT per 10^8 A/cm^2 of applied current.

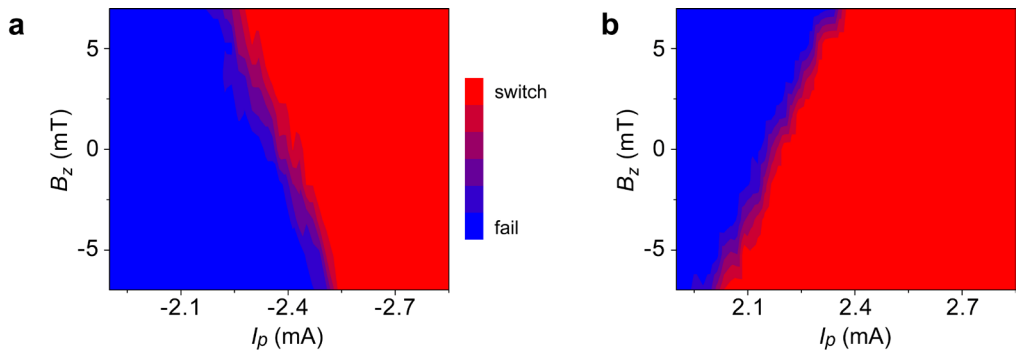

Figure S6. a, Average of M_z for a 500 nm Co dot after the injection of twenty positive current pulses as a function of pulse amplitude and perpendicular field component. **b,** Same as **a** for negative current pulses. Red (blue) indicates that 100% (0%) of the magnetization has switched.

5. Effect of top layer oxidation: magnetic stability vs. switching current

The magnetocrystalline anisotropy of AlO_x/Co/Pt systems is known to depend critically on the degree of oxidation at the Co-Al interface[1,2], whereas the Rashba splitting at the surface of ferromagnetic metals has been shown to vary strongly with oxidation[7]. The correlation between magnetocrystalline anisotropy, oxidation, and Rashba interaction can be used to shed light on the origin of the switching effect.

To this end, we have fabricated AlO_x/Co/Pt dots with different degrees of Al oxidation. In order to minimize differences due to the quality of the substrate, Pt layer, and Co/Pt interface, we have grown a flat Co(0.6 nm)/Pt(3 nm) layer on a single wafer, covered it with an Al wedge (1.6 – 2.1 nm), and oxidized it for 30s. Samples patterned on regions with larger (smaller) Al thickness were thus less (more) oxidized. Representative magnetization curves of this series of dots are reported in Fig. S7, where labels S1-7, S1-8, S1-10 indicate samples with increasing oxidation of the top layer with nominal Al thickness between 1.70 and 1.75 nm. As expected, the easy axis coercivity (Fig. S7a) and the in-plane magnetic field required to tilt the magnetization away from the easy axis (Fig. S7b) are larger in the more oxidized dots.

The switching curves for samples 1-10, 1-8, and 1-7 are reported in Fig. S8 for θ = 90º and Fig. S9 for θ = 88º. We observe that, even though the samples with a higher degree of oxidation have a stronger anisotropy, their magnetization switches at lower current. For example, full switching in the entire field range spanned by the coercivity of each dot is

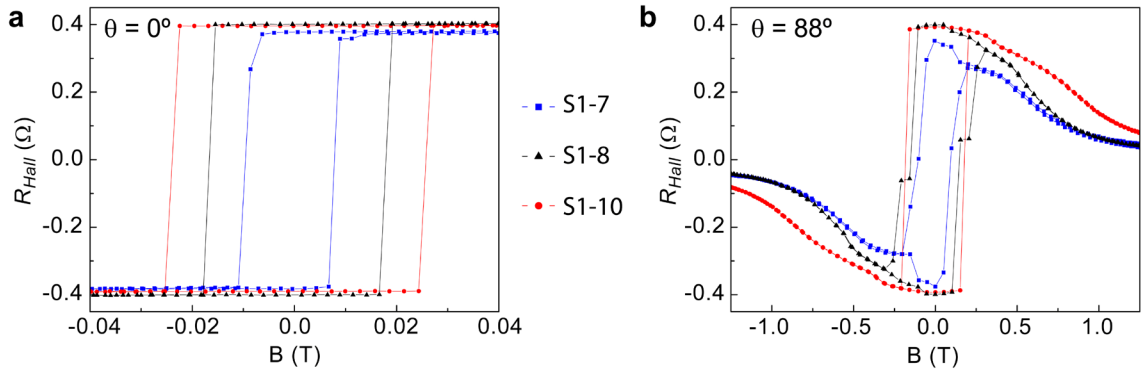

Figure S7. a, M_z measured as a function of magnetic field applied parallel to the easy axis (θ = 0º) and **b,** close to the hard plane direction (θ = 88º) for samples 1-7, 1-8, 1-10.

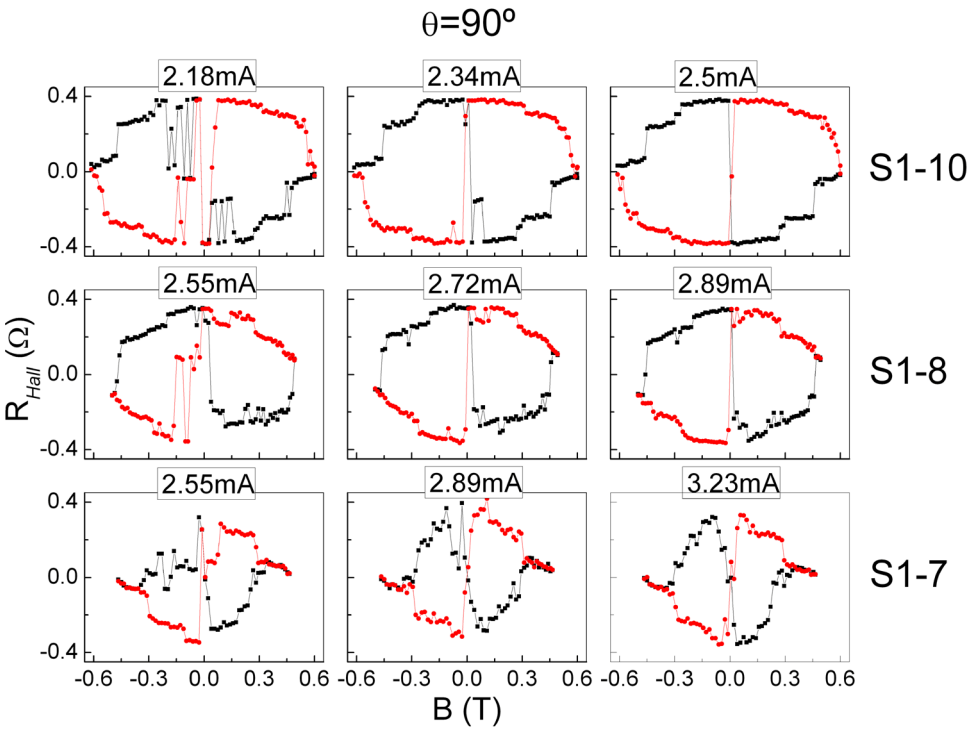

Figure S8. a, Current-induced switching of samples 1-7, 1-8, 1-10 measured by the anomalous Hall resistance after injection of positive (black squares) and negative (red circles) current pulses of variable amplitude. The magnetic field is in-plane ($\theta = 90^\circ$, $\phi = 0^\circ$).

achieved at 2.5 mA in sample 1-10 and 3.2 mA in sample 1-7 when the field is perfectly planar (Fig. S8, $\theta = 90^\circ$). These values increase slightly when the field is tilted off-plane (Fig. S9, $\theta = 88^\circ$), as expected due to the presence of a finite B_z. We note that the differences of the threshold currents required for switching from one sample to another are too large to be attributed to differences of the Al thickness. Therefore, we conclude that oxidation of the top layer enhances the value of the effective switching field.

Besides its fundamental implications, this result has important consequences for applications. One of the main problems to reduce the bit size of magnetic memories is represented by the need to use high anisotropy materials to overcome the superparamagnetic limit, which makes it increasingly hard to write such bits. Our data show that the hardest magnetic dots, those with larger magnetic anisotropy, switch more

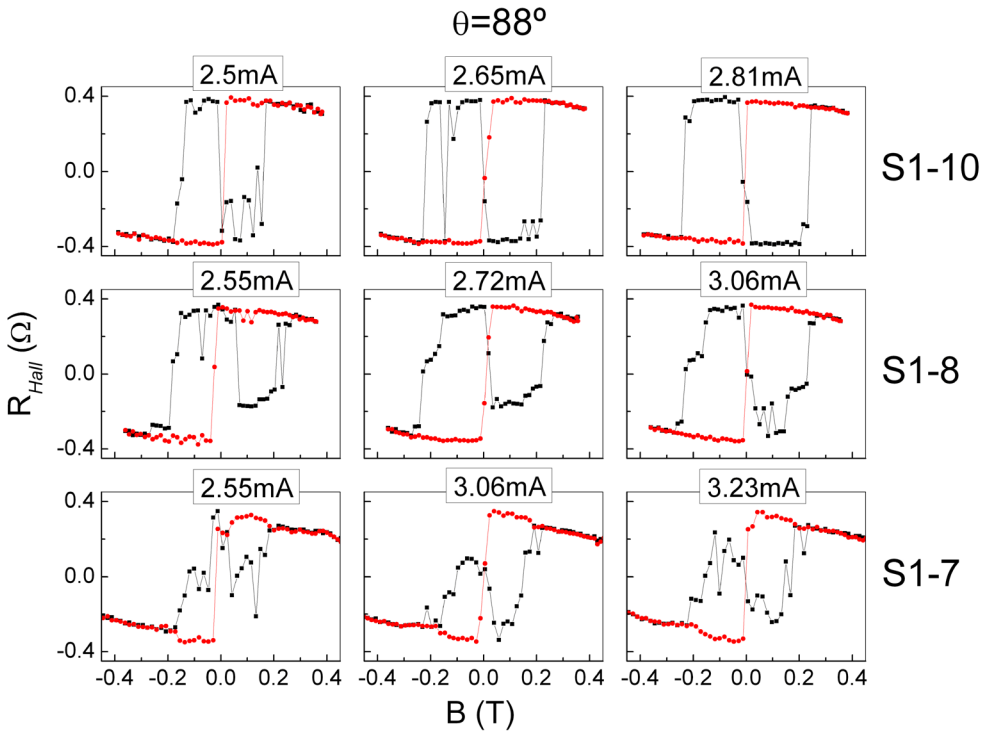

Figure S9. a, Current-induced switching of samples 1-7, 1-8, 1-10 measured by the anomalous Hall resistance after injection of positive (black squares) and negative (red circles) current pulses of variable amplitude. The magnetic field is tilted 2° off-plane ($\theta = 88°$, $\phi = 0°$).

easily than the soft ones, providing a solution to the long-standing antagonism between magnetic stability and writability.

6. Discussion of spin-orbit torques

We provide here a comparative discussion of the possible contributions to the spin-orbit torque that gives rise to the switching field described in the manuscript. Experimentally, we measure an effect that has the symmetry of the cross product $\mathbf{B}_\mathbf{R} \times \mathbf{B}$. However, the external field in a ferromagnet has negligible influence on the spin polarization of the conduction electrons compared to the internal exchange field due to the local magnetization. Thus the intrinsic symmetry of the switching field must be $\mathbf{B}_\mathbf{R} \times \mathbf{M}$,

where the direction of **M** is determined by the external field **B**. Within this hypothesis, the switching field is equivalent to a torque pointing along $\mathbf{B_R}$. When the magnetization is at remanence (pointing either up or down) the direction of the effective switching field is in-plane, either parallel or antiparallel to the current. In the absence of an applied field, the current will destabilize both the up and down directions of **M**. On the other hand, when a field is applied parallel to the current, the effective switching field either adds or subtracts to the external field, thereby destabilizing one direction and stabilizing the other. We discuss below different spin-orbit torque terms that may induce an effective field having this symmetry.

6.1 Spin Hall Effect

The spin Hall effect (SHE) induced by current injection in the thin Pt layer underneath the Co dot generates a vertical spin current that can be absorbed by the Co layer. The absorption of this spin current is equivalent to a change of angular momentum, which creates a torque along the *y* direction that has the same symmetry as the effect reported here.

The ratio between the vertical spin current and the horizontal charge current is given by the value of the spin Hall angle α_{SH}. Besides this parameter, the amplitude of the vertical spin current is also conditioned by the thickness of the nonmagnetic layer: in order to reach maximum amplitude at the top and bottom interfaces, the thickness must be greater than the spin diffusion length λ_{SF}. The SHE has been intensively investigated in Pt in recent years. Values reported for the spin Hall angles in Pt range between α_{SH} = 0.004 and 0.076 (Refs. 8-11). Reports on the spin diffusion length yield λ_{SF} = 3 - 14 nm (Refs. 8-12).

Using these values we can estimate the maximum torque exerted on the Co magnetization by the absorption of the spin current induced by the SHE in the Pt layer. Supposing that all the spin current is injected and absorbed in the Co layer, the corresponding change of magnetization is given by $\frac{dM}{dt} = \frac{1}{t}\alpha_{SH} j \frac{\mu_B}{e}$, where t is the thickness of the magnetic layer, μ_B= 9.27 x 10^{-24} J/T, and e = 1.6 10^{-19} C. Using

$\frac{dM}{dt} = -\gamma M B_{SH}$, where $\gamma = 1.76\ 10^{11}$ s^{-1} T^{-1}, we estimate an equivalent magnetic field $B_{SH} = \frac{\alpha_{SH} j \mu_B}{t \cdot \gamma \cdot M \cdot e}$. Taking $\alpha_{SH} = 0.076$, $M = 8.7\ 10^5$ A/m, and $t = 0.6$ nm, we obtain $B_{SH} = 47$ mT for $j = 10^8$ A/cm^2. This value must be multiplied by a factor $j_S(t_{Pt}) / j_S(\infty) = 1 - \mathrm{sech}(t_{Pt} / \lambda_{sf})$, which takes into account the fact that, owing to the finite spin diffusion length of Pt, the spin current from the top Pt interface is partially compensated by a spin current of opposite sign from the bottom interface[11]. The minimum correction is obtained for $\lambda_{SF} = 3$ nm, which gives $j_S(t_{Pt}) / j_S(\infty) = 0.35$. The maximum contribution of the SHE, assuming 100% transparency of the Pt/Co interface, thus corresponds to $B_{SH} = 16$ mT for $j = 10^8$ A/cm^2, which is approximately 5 times smaller compared to the effective switching field estimated in Sect. 4.

The measurements reported in Sect. 5 for samples with different degrees of Al oxidation further support the hypothesis that the mechanism responsible for switching is different from the SHE described above. Samples 1-7 to 1-10 were grown on the same wafer and have therefore identical Pt and Co thickness, structure, and Pt/Co interface properties. Thus, the torque produced by the SHE is expected to be the same across this series of samples. If the torque produced by the SHE would be the main cause of switching, we would expect the softer samples to switch well before the harder ones, contrary to our observations. We cannot exclude, however, that a more complex form of SHE than reported thus far is at work in our case, possibly enhanced by the Rashba field at the Co interface.

6.2. Out-of-plane spin polarization: Analogy with spin accumulation observed in nonmagnetic semiconductors

Besides the possibility of inducing a torque via the spin current originating from the Pt underlayer discussed in the previous paragraph, theoretical models of the Rashba effect in nonmagnetic semiconductors suggest an alternative explanation for the switching field.

We provide here a qualitative explanation of the origin of perpendicular spin polarization arising from parallel in-plane current and magnetic field in a nonmagnetic two-dimensional electron gas (2DEG), according to the work of Engel, Rashba, and Halperin[13].

Finally, we discuss the analogy with phenomena taking place in a ferromagnetic metal layer and highlight the need of a quantitative dynamic theory to describe the switching of a perpendicularly magnetized thin film by an in-plane current.

According to the Rashba model of a 2DEG with structure inversion asymmetry along **z**[14], an electric current in the **x** direction induces homogenous spin polarization of the charge carriers parallel to **y**, equivalently to an effective spin-orbit field $\mathbf{B_R} = \alpha_R (\mathbf{z} \times \mathbf{j})$, where α_R is the Rashba constant and **j** the current density vector. This is the origin of the effective transverse magnetic field, parallel to **y**, predicted[15] and observed previously in FM[4,16]. In addition to spin accumulation parallel to **y**, Faraday measurements of nonmagnetic InGaAs heterostructures revealed that a magnetic field **B** applied in-plane collinear to the current induces a perpendicular spin polarization component $\mathbf{s_z}$[17]. Engel, Rashba, and Halperin provided a theoretical model for this effect in a 2DEG, showing that $\mathbf{s_z}$ arises from the combination of $\mathbf{B_R}$ with anisotropic spin-dependent conductivity induced by impurity scattering or/and nonparabolic electron band dispersion[13]. Schematically, this effect may be understood as follows: if only the Rashba interaction is considered, nonequilibrium spin accumulation $\boldsymbol{s_R}$ is created in the direction of $\mathbf{B_R}$, transverse to the current (Fig. S10a). A magnetic field **B** // **j**, also induces spin accumulation $\boldsymbol{s_B}$, independently from $\mathbf{B_R}$ and parallel to **j** (Fig. S10b). The spins oriented along $\mathbf{B_R}$ now precess around **B** and vice versa. If the external and Rashba fields can be treated on equal footings, since $\boldsymbol{s_B}$ and $\boldsymbol{s_R}$ are respectively proportional to **B** and $\mathbf{B_R}$, the two precessional torques $\mathbf{B_R} \times \mathbf{s_B}$ and $\mathbf{B} \times \mathbf{s_R}$ are equal and opposite in sign, cancelling each other, as shown by the green dashed arrows in Fig. S10b. In such a case the resultant spin accumulation can only lie in-plane along the average field $\mathbf{B} + \mathbf{B_R}$. Yet this is a too simple picture, as $\mathbf{B_R}$ is not a true magnetic field but rather an *effective* field proportional to the electron mobility. Consider the nonzero spin polarization induced by **B** along **x** as being the sum of a "majority" and "minority" component: $\mathbf{s_B} = \mathbf{s_B^+} + \mathbf{s_B^-}$. If $\mathbf{s_B^+}$ and $\mathbf{s_B^-}$ electrons scatter at unequal rates, their mobility differs. The Rashba fields $\mathbf{B_R^+}$ and $\mathbf{B_R^-}$ experienced by $\mathbf{s_B^+}$ and $\mathbf{s_B^-}$ are not equal and the two spin populations rotate around **y** with different speed, no

longer compensating the perpendicular torque arising from the $\mathbf{B}\times\mathbf{s}_\mathbf{R}$ term (Fig. S10c). Taking into account spin relaxation, it can be shown that this gives rise to a stationary perpendicular spin accumulation component $\mathbf{s}_z \sim \mathbf{B}_\mathbf{R}\times\mathbf{B}$ (Ref. 13).

In a ferromagnet, the term $\mathbf{B}_\mathbf{R}\times\mathbf{B}$ is replaced by $\mathbf{B}_\mathbf{R}\times\mathbf{M}$ since the role of the external field in inducing spin accumulation parallel to **j** is played by the Co magnetization (**M**) through the *s-d* exchange interaction. This term has the symmetry required to model the current-induced effective field responsible for the switching of AlO_x/Co/Pt films. Moreover, the switching efficiency increases with current amplitude and external field, in agreement with the above model. The analogy between our observations and the theory of Ref. 13 can be carried further by noting that strong Rashba fields can be induced in this material[4,16] and that the mobility of the conduction electrons in Co is strongly spin-dependent[18]. Because of the filled character of the majority band in Co, the mobility of $\mathbf{s}_\mathbf{B}^+$ spins is now much larger compared to $\mathbf{s}_\mathbf{B}^-$. As $\mathbf{B}_\mathbf{R}^+\times\mathbf{s}_\mathbf{B}^+ \gg \mathbf{B}_\mathbf{R}^-\times\mathbf{s}_\mathbf{B}^-$, the conduction electrons accumulate a steady state spin polarization parallel to $\mathbf{B}_\mathbf{R}\times\mathbf{M}$. An in-plane external field is required to tilt the magnetization and produce a finite in-plane component $\mathbf{M}_\mathbf{x}$ // **B**, **j**, which results in out-of-plane spin accumulation finally exerting a downward or upward effective field on **M** depending on the sign of current and applied field.

We remark that the dynamics of the switching process is not included in such a schematic model, in particular effects due to the simultaneous presence of Rashba and perpendicular effective field, Gilbert damping, as well as Joule heating by the current

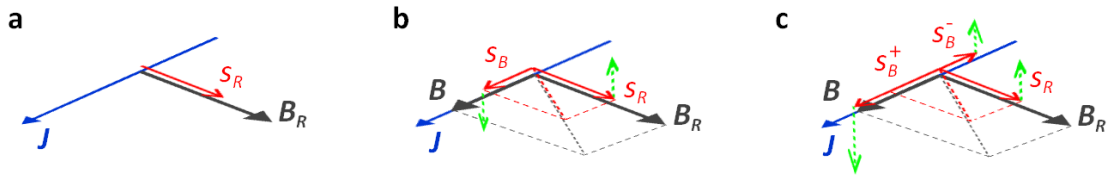

Figure S10. a, Rashba effective magnetic field $\mathbf{B}_\mathbf{R}$, and induced transverse spin polarization $\mathbf{s}_\mathbf{R}$. **b,** Spin polarization $\mathbf{s}_\mathbf{B}$ induced by a magnetic field collinear to the current. Green dashed arrows indicate torques acting on $\mathbf{s}_\mathbf{R}$ and $\mathbf{s}_\mathbf{B}$. **c,** Different torques act on the majority ($\mathbf{s}_\mathbf{B}^+$) and minority ($\mathbf{s}_\mathbf{B}^-$) components of $\mathbf{s}_\mathbf{B}$, producing a net uncompensated perpendicular torque.

pulses. Nonetheless, all the key aspects of our measurements are reproduced. A quantitative theory of this effect in ferromagnetic metals must necessarily take into account the enhanced Rashba interaction as well as the strong *s-d* exchange coupling compared to Zeeman field splitting in semiconductors. These factors, together with significantly smaller spin relaxation times, are expected to induce orders of magnitude larger spin accumulation in ferromagnets.

Finally, the theory of Engel, Rashba and Halperin predicts that crossed **B** and $\mathbf{B_R}$ fields induce an oscillating perpendicular spin polarization component in addition to the stationary one. Both static and dynamic components have been observed by Faraday rotation measurements in InGaAs[17]. The dynamic component has been shown to oscillate with a period of a few ns, although its amplitude relative to the steady state spin polarization has not been quantified. We note that, regardless on the relative intensity of these two components, a dynamic component of the effective perpendicular field would not be observed in our experiment due to the very different energy scales involved with respect to semiconductors. While the Rashba interaction is about two orders of magnitude larger than in semiconductors, the role of the external field is now played by the effective *s-d* exchange field, also orders of magnitude larger compared to the applied field in the semiconductor experiment. Since the timescale of any physical process is dictated by the magnitude of the corresponding energy, the oscillations observed in semiconductors are expected to be much faster in metals. In our samples these oscillations should occur with a period of the order of 10 ps. Because the pulses that we use in our experiments are much longer (15 ns) than the oscillation period, only the quasi-static component of the out-of-plane effective field can have measurable effects.

To summarize, the symmetry of the switching effect reported here is in agreement with spin-orbit torques created either by a vertical spin current or by the combination of Rashba effect and spin dependent mobility. The fact that the SHE in the Pt underlayer is too weak to account for the efficiency of the switching field and that magnetically harder samples (with higher degree of top layer oxidation) switch at lower current compared to softer ones, suggest that a complex mechanism is at work where the Rashba effect plays a

role, either by significantly enhancing the SHE or by inducing steady-state perpendicular spin accumulation in a system with strong spin-dependent conductivity.

7. References

1. Monso, S. Rodmacq, B. Auffret, S. Casali, G. Fettar, F. Gilles, B. Dieny, B. & Boyer, P. Crossover from in-plane to perpendicular anisotropy in Pt/CoFe/AlOx sandwiches as a function of Al oxidation: A very accurate control of the oxidation of tunnel barriers. *Appl. Phys. Lett.* **80**, 4157-4159 (2002).

2. Nistor, L. E. Rodmacq, B. Auffret, S. & Dieny B., Pt/Co/oxide and oxide/Co/Pt electrodes for perpendicular magnetic tunnel junctions, *Appl. Phys. Lett.* **94**, 012512 (2009).

3. Rodmacq, B. Manchon, A. Ducruet, C. Auffret, S. & Dieny, B. Influence of thermal annealing on the perpendicular magnetic anisotropy of Pt/Co/AlO_x trilayers. *Phys. Rev. B* **79**, 024423 (2009).

4. Miron, I. M. Gaudin, G. Auffret, S. Rodmacq, B. Schuhl, A. Pizzini, S. Vogel, J. & Gambardella, P. Current-driven spin torque induced by the Rashba effect in a ferromagnetic metal layer. *Nat. Mater*. **9**, 230 (2010).

5. Koch, R. H. Katine, J. A. & Sun, J. Z. Time-Resolved Reversal of Spin-Transfer Switching in a Nanomagnet. *Phys. Rev. Lett.* **92**, 088302 (2004).

6. Yagami, K. Tulapurkar, A. A. Fukushima, A. & Suzuki, Y. Inspection of Intrinsic Critical Currents for Spin-Transfer Magnetization Switching. *IEEE Trans. Mag.* **41**, 2615 (2005).

7. Krupin, O. *et al.* Rashba effect at magnetic metal surfaces. *Phys. Rev. B* **71,** 201403(R) (2005).

8. Kimura, T. Otani, Y. Sato, T. Takahashi, S. & Maekawa, S. Room-Temperature Reversible Spin Hall Effect. *Phys. Rev. Lett.* **98**, 156601 (2007).

9. Ando, K. Takahashi, S. Harii, K. Sasage, K. Ieda, J. Maekawa, S. & Saitoh, E. Electric Manipulation of Spin Relaxation Using the Spin Hall Effect. *Phys. Rev. Lett.* **101**, 036601 (2008).

10. Mosendz, O. Vlaminck, V. Pearson, J. E. Fradin, F. Y. Bauer, G. E. W. Bader, S. D. & Hoffmann A. Detection and quantification of inverse spin Hall effect from spin pumping in permalloy/normal metal bilayers. *Phys. Rev. B* **82**, 214403 (2010).

11. Liu, L. Moriyama, T. Ralph, D. C. & Buhrman, R. A. Spin-Torque Ferromagnetic Resonance Induced by the Spin Hall Effect. *Phys. Rev. Lett.* **106**, 036601 (2011).

12. Vila, L. Kimura, T. & Otani, Y. Evolution of the Spin Hall Effect in Pt Nanowires: Size and Temperature Effects. *Phys. Rev. Lett.* **99**, 226604 (2007).

13. Engel, H.-A. Rashba, E. I. & Halperin, B.I. Out-of-Plane Spin Polarization from In-Plane Electric and Magnetic Fields. *Phys. Rev. Lett*. **98**, 036602 (2007).

14. Bychkov, Yu.A. & Rashba, E. I. Properties of a 2D electron gas with lifted spectral degeneracy. *J. Exp. Theor. Phys. Lett.* **39**, 78-81 (1984).

15. Manchon, A. & Zhang, S. Theory of nonequilibrium intrinsic spin torque in a single nanomagnet. *Phys. Rev. B* **78**, 212405 (2008).

16. Pi, U. H. Kim, K. W. Bae, J. Y. Lee, S. C. Cho, Y. J. Kim, K. S. & Seo, S. Tilting of the spin orientation induced by Rashba effect in ferromagnetic metal layer. *Appl. Phys. Lett.* **97**, 162507 (2010).

17. Kato, Y.K. Myers, R.C. Gossard, A.C. & Awschalom, D.D. Current-induced spin polarization in strained semiconductors. *Phys. Rev. Lett.* **93**, 176601 (2004).

18. Campbell, A. & Fert, A. Transport properties of ferromagnets, in Ferromagnetic Materials Vol. 3, E. P. Wohlfart Ed., North Holland (Amsterdam, 1982).